ELSEVIER

Thermochimica Acta 275 (1996) 235–247

thermochimica acta

Solid–solid interaction in the pure and Li_2O-doped MoO_3–Al_2O_3 system

G.A. El-Shobaky [a,*], F.H.A. Abdalla [b], A.M. Ghozza [c], K.A. Khalil [c]

[a] *National Research Centre, Dokki, Cairo, Egypt*
[b] *Central Metallurgical Research and Development Institute (CMRDI), Cairo, Egypt*
[c] *Chemistry Department, Faculty of Science, Zagazig University, Zagazig, Egypt*

Received 20 March 1995; accepted 5 August 1995

Abstract

The effects of Li_2O doping (1.5 and 6 mol%) on solid–solid interactions and the phase transformation process in the MoO_3–Al_2O_3 system were investigated using thermogravimetry, differential thermal analysis and X-ray diffraction (TG, DTA and XRD) techniques. The proportions of molybdena expressed as wt% MoO_3 were 22 and 41.4.

The results obtained revealed that MoO_3 interacted with Al_2O_3 at temperatures starting from 500°C, forming orthorhombic $Al_2(MoO_4)_3$; doping with lithium oxide was found to promote the reaction. The complete transformation of molybdenum trioxide into aluminium molybdate required heating of the mixed oxides at 700°C. The molybdate produced decomposed at temperatures above 800°C yielding α-Al_2O_3 and MoO_3. The Li_2O doping enhanced the crystallization of α-alumina and retarded the thermal decomposition of $Al_2(MoO_4)_3$. The MoO_3 produced partly sublimed and the remaining portion dissolved in the alumina matrix forming an MoO_3–Al_2O_3 solid solution. Li_2O doping increased the amount of MoO_3 sublimed at 900–1100°C to an extent proportional to the concentration of the dopant. In other words, Li_2O treatment decreased the solubility of MoO_3 in Al_2O_3. The promoting effect of Li_2O on $Al_2(MoO_4)_3$ formation at 500°C was attributed to dissolution of a small portion of Li_2O in the MoO_3 lattice, with subsequent increase in the mobility of Mo^{6+} ions. The possible increase in the mobility of these ions might also account for the observed decrease in the solubility of MoO_3 in Al_2O_3.

Keywords: Catalysis; Doping; DTA; Solid–solid interactions; TG; XRD

* Corresponding author.

SSDI 0040-6031(95)02694-0

1. Introduction

Molybdenum oxides loaded on an active Al_2O_3 support are one of the most important solid catalysts [1–5]. Molybdenum may exist as isolated MoO_4^{2-} species, dispersed oxomolybdate patches, and also as MoO_3 or $Al_2(MoO_4)_3$ compound [5–7]. The identification of the different chemical states of molybdenum requires extensive studies using, for example, XRD, ESR DRS, XPS and laser Raman spectroscopy techniques [1–5]. The supported catalysts are usually prepared by impregnation of an alumina support from an aqueous solution of ammonium molybdate followed by thermal treatment at suitable temperatures.

The heating of a physical mixture of crystalline MoO_3 and γ-alumina at 400°C for about 24 h resulted in the disappearance of all X-ray diffraction lines of the MoO_3 phase [6–10]. This behaviour has been attributed to monolayer dispersion of molybdenum trioxide on the surface of the Al_2O_3 support. The increase in calcination temperature of MoO_3–Al_2O_3 up to 600°C enhances the surface and bulk mobilities of the MoO species leading to the formation of well-crystallized MoO_3 or $Al_2(MoO_4)_3$ compounds [8]. Further increase in the calcination temperature to 800–900°C resulted in thermal decomposition of the aluminium molybdate into MoO_3 and Al_2O_3. It was reported in our previous investigation that unloaded MoO_3 volatilized on heating at 800°C and, when supported on a poorly crystalline γ-Al_2O_3 and heated at 800–1000°C, a portion of the MoO_3 volatilized and the rest dissolved in the Al_2O_3 matrix forming MoO_3–Al_2O_3 solid solution [11]. The metal-support interactions in the MoO_3–Al_2O_3 system could be influenced by doping with certain foreign cations such as Li^+, Zn^{2+}, Ga^{3+} and Ge^{4+} [3,4].

The present investigation reports a study on the effect of Li_2O doping on solid–solid interaction in the MoO_3–Al_2O_3 system using TG, DTA and X-ray diffraction techniques. These techniques allowed us to clarify the effects of Li_2O doping on the thermal behaviour of ammonium molybdate supported on Al_2O_3, and to identify the different phases produced by heating the mixed solids at various temperatures.

2. Experimental

2.1. Materials

A known mass of $Al(OH)_3$, analytical grade supplied by Prolabo, was impregnated with ammonium paramolybdate (BDH) solutions containing two different proportions of $(NH_4)_6Mo_7O_{24}.4H_2O$. The proportions of ammonium molybdate were calculated so that the molar compositions of the calcined materials were 0.2 $MoO_3:Al_2O_3$ and 0.5 $MoO_3:Al_2O_3$. The impregnated materials were dried at 120°C, then calcined at 500, 700, 800, 900 and 1000°C. The lithium oxide doping was effected by treating the dried impregnated materials with an aqueous $LiNO_3$ solution prior to the calcination. The time of heating of pure and doped materials was fixed at 5 h, and the amounts of lithium were 1.5 and 6.0 mol% Li_2O, respectively (with respect to the sum of Al_2O_3 and MoO_3). The prepared mixed solid specimens were designated AlMo-I, AlMo-I–1.5Li, AlMo-I–6Li, AlMo-II, AlMo-II–1.5Li and AlMo-II–6Li. The nominal molar compositions of the calcined mixed solids were 0.2 MoO_3:Al_2O_3 (I) and 0.5 MoO_3:Al_2O_3 (II) and contained 22 and 41.4 wt% MoO_3, respectively. $Al(OH)_3$ was used as a starting support material due to its decomposition during the thermal transformation of molybdate (into molybdena) which may provide chances for solid–solid interactions that must not be attainable on using Al_2O_3 as a support.

2.2. Techniques

DTA and TG analyses of various uncalcined materials were carried out using a Netzsch–Gerätebau simultaneous thermal analysis apparatus (STA 409, type 6.223). The rate of heating was kept at 10°C min^{-1} and the analyses were followed at temperatures between room temperature and 1100°C. A 100 mg sample of each solid specimen was employed in each case.

An X-ray investigation of the thermal products of the different pure and doped mixed solids was performed with a Philips diffractometer (type PW 1390). The patterns were run with nickel-filtered copper radiation ($\lambda = 1.5405$ Å) at 36 kV and 16 mA with scanning speed 2° min^{-1}.

3. Results and discussion

3.1. Thermal behaviour of pure and doped materials

DTA and TG curves of various pure and doped materials were determined and results obtained are summarized in Tables 1 and 2. Representative DTA and TG curves are illustrated in Figs. 1 and 2 for AlMo-I and AlMo-II doped with 6 mol% Li_2O. The DTA curves of pure and doped solids exhibited six sets of endothermic peaks. The first set of peaks are weak and broad, located at about 100°C, indicating the loss of physisorbed water. The second set of peaks are sharp with their maxima found at 189–234°C, indicating the thermal decomposition of ammonium molybdate into molybdenum oxide(s) [11]. The third set of peaks are the most sharp and strong, having their maxima at 294–314°C, characterizing the thermal decomposition of $Al(OH)_3$ into Al_2O_3 [10,12]. The fourth set of peaks, relatively strong and broad, at 468–510°C, might correspond to removal of the OH groups bound to the alumina matrix [13]. In fact, it has been shown that the complete dehydroxylation of Al_2O_3 requires prolonged heating of the materials at temperatures above 450°C [13, 14] or subjecting Al_2O_3 to gamma-irradiation [15]. The fifth set of endothermic peaks, relatively strong and sharp, observed at 790–950°C might indicate sublimation of molybdenum oxide(s) [11]. The sixth set of endothermic peaks, strong and sharp, detected at 990–1012°C might correspond to volatilization of molybdenum oxide. In fact these peaks were accompanied by significant weight losses.

Inspection of the results given in Table 2 show that:

(i) The calculated weight losses accompanying the thermal decomposition of AlMo-I and AlMo-II materials to the corresponding oxides (alumina and molybdena)

Table 1
DTA results for pure and doped materials

Solid	DTA/$\Delta T/T$	T_{max}/°C
AlMo-I	endo, w	95
	endo, s	189
	endo, vs	296
	endo, w	468
	endo, w	890
	endo, s	1004
AlMo-I–1.5Li	endo, w	93
	endo, s	193
	endo, vs	290
	endo, w	479
	endo, w	940
	endo, s	998
AlMo-I-6Li	endo, w	101
	endo, s	239
	endo, vs	294
	endo, w	497
	endo, w	920
	endo, s	991
AlMo-II	endo, w	92
	endo, s	205
	endo, vs	310
	endo, w	492
	endo, w	869
	endo, s	1012
AlMo-II–1.5Li	endo, w	102
	endo, s	223
	endo, vs	300
	endo, w	500
	endo, w	935
	endo, s	1012
AlMo-II–6Li	endo, w	95
	endo, s	217
	endo, vs	313
	endo, w	464
	endo, s	986
	endo, s	1012

Key: w = weak, s = strong, vs = very strong peaks.

are 27.2 and 25.1%, respectively. These values are smaller than those found for different pure and doped solids during the thermal treatment at temperatures ranging between 100 and 800°C. This difference suggests the sublimation of a portion of the MoO_3 solid produced.

(ii) The calculated weight losses accompanying the complete sublimation of MoO_3 in AlMo-I and AlMo-II solids are 43.1 and 56.1%, respectively. The comparison of

Table 2
TG results of pure and doped materials

Solid	100–800°C %	990–1020°C %	Calculated %	100–1100°C %	Calculated %	Wt.% MoO_3 dissolved[a]
AlMo-I						
0.0 Li_2O	32.3	3.7	27.2	36	43.1	7.1
1.5 Li_2O	30.0	7.8	–	38	-	5.1
6 Li_2O	31.3	9.5	–	40.6	...	2.5
AlMo-II						
0.0 Li_2O	31.7	5.2	25.1	37	56.1	19.1
1.5 Li_2O	25.3	18.7	–	44.5	–	11.6
6 Li_2O	28.0	19.5	–	46.2	–	9.9

[a] The data of this column were computed by subtracting the data of column 5 from those given in column 6.

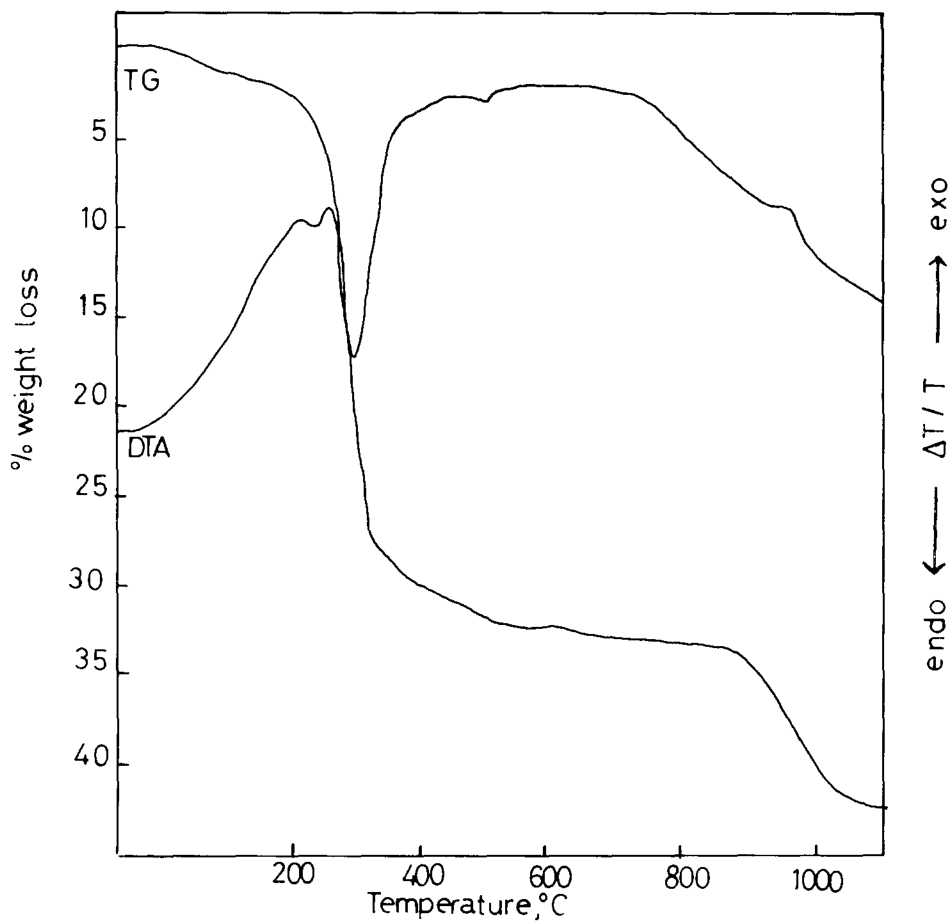

Fig. 1. DTA and TG curves of uncalcined AlMo-I doped with 6 mol% Li_2O.

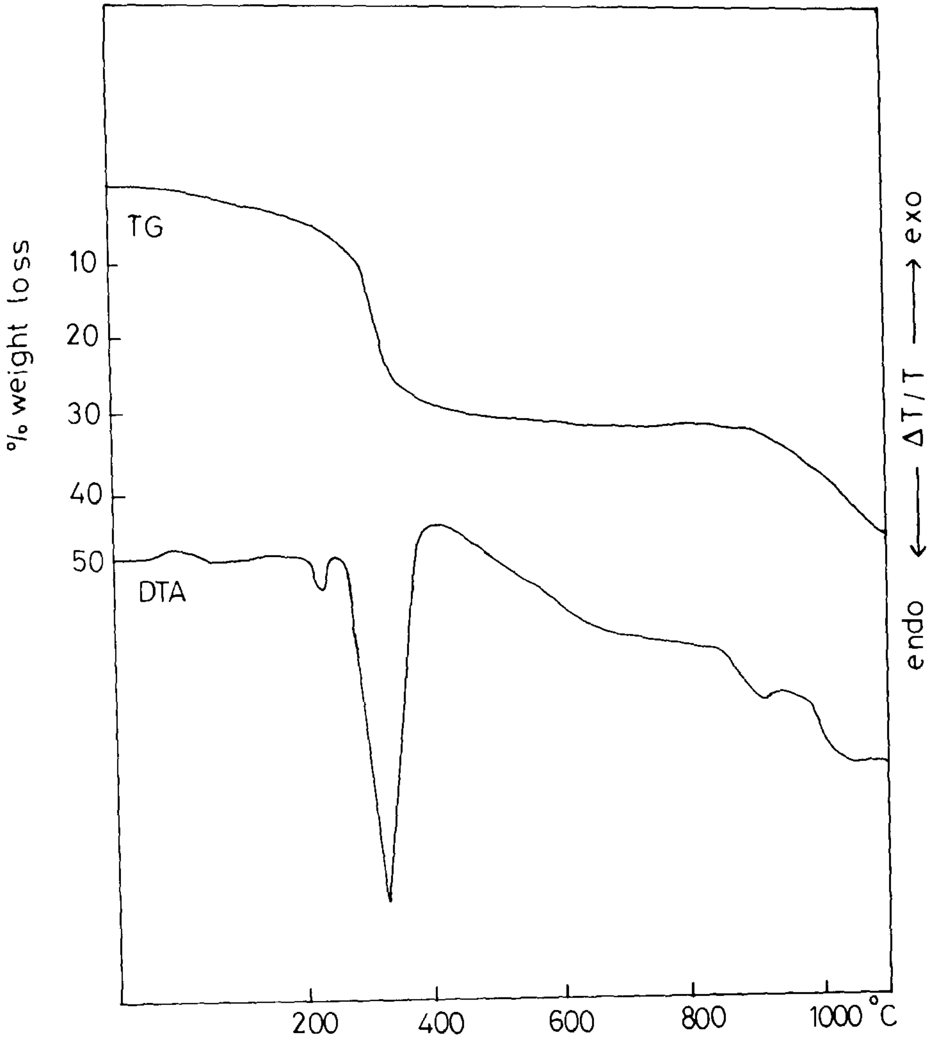

Fig. 2. DTA and TG curves of uncalcined AlMo-II doped with 6 mol% Li_2O.

these values with those found (100–1100°C) clearly indicates volatilization of a portion of the MoO_3 present and dissolution of the other portion. These results enable us to calculate the amounts of MoO_3 dissolved in pure and Li_2O-doped materials. These results indicate that lithium oxide doping decreases the solubility of molybdenum trioxide in the alumina matrix to an extent proportional to the amount of Li_2O present.

3.2. XRD of calcination products

Preliminary experiments showed that the thermal decomposition of ammonium molybdate in air at 500–700°C resulted in the formation of well-crystallized orthorhombic MoO_3 which sublimes completely by heating at 800°C. However, the thermal products of $Al(OH)_3$ at 500 or 700°C are amorphous in nature, while the solid preheated at 1000°C consists of crystallized κ-alumina together with a minute amount of α-Al_2O_3 [6,10]. The complete transformation of the pure alumina specimen into the α-form required thermal treatment at elevated temperatures, > 1200°C [10,13,16], or the presence of certain foreign oxides such as NiO [12], V_2O_5 [17], Co_3O_4 [18] and CuO [19]. These oxides catalyse the crystallization process of alumina into the α-corundum phase.

XR diffractograms of pure and doped mixed solids preheated in air at 500, 700, 800, 900 and 1000°C were determined. Table 3 lists the different phases present in pure and doped mixed solids preheated at 500–1000°C. The results obtained showed that pure and doped AlMo-I solids preheated at 500°C were amorphous in nature. The diffraction lines of orthorhombic MoO_3 and $Al_2(MoO_4)_3$ phases were detected in the diffractograms of pure and doped AlMo-II specimens calcined at 500°C. The intensity

Table 3
Crystalline phase compositions of the calcined products detected by XRD

Solid	Calcination temperature/°C	Crystalline composition
AlMo-I	500	–
AlMo-I–1.5%Li_2O	500	Poorly crystalline γ-Al_2O_3
AlMo-I–6%Li_2O	500	Poorly crystalline γ-Al_2O_3
AlMo-II	500	MoO_3, poorly crystalline γ-Al_2O_3 and $Al_2(MoO_4)_3$
AlMo-II–1.5%Li_2O	500	MoO_3, poorly crystalline γ-Al_2O_3 and $Al_2(MoO_4)_3$
AlMo-II–6%Li_2O	500	MoO_3, poorly crystalline γ-Al_2O_3 and $Al_2(MoO_4)_3$
AlMo-I	700	$Al_2(MoO_4)_3$, κ- and γ-aluminas
AlMo-I–1.5%Li_2O	700	Aluminium molybdate together with κ- and γ-Al_2O_3
AlMo-I–6%Li_2O	700	$Al_2(MoO_4)_3$, κ- and γ-aluminas, and $LiAl_5O_8$
AlMo-II	700	$Al_2(MoO_4)_3$ and δ-Al_2O_3
AlMo-II–1.5%Li_2O	700	Aluminium molybdate and κ- alumina
AlMo-II–6%Li_2O	700	$Al_2(MoO_4)_3$, κ-Al_2O_3 and $LiAl_5O_8$
AlMo-I	800	$Al_2(MoO_4)_3$ (small amount), κ- and γ-Al_2O_3, together with minute amount of α-alumina
AlMo-I–1.5%Li_2O	800	$Al_2(MoO_4)_3$, γ-, θ-Al_2O_3, and well-crystallized α-Al_2O_3
AlMo-I–6%Li_2O	800	α-Al_2O_3, $Al_2(MoO_4)_3$ and θ-Al_2O_3
AlMo-II	800	Small amount of $Al_2(MoO_4)_3$, δ- and κ-Al_2O_3
AlMo-II–1.5%Li_2O	800	$Al_2(MoO_4)_3$, κ-Al_2O_3, and well-crystallized α-Al_2O_3
AlMo-II–6%Li_2O	800	$Al_2(MoO_4)_3$, well-crystallized α-Al_2O_3 and Li_3MoO_5
AlMo-I	900	α-Al_2O_3
AlMo-I–1.5%Li_2O	900	α-Al_2O_3
AlMo-I–6%Li_2O	900	α-Al_2O_3 and Li_4MoO_5
AlMo-II	900	α-Al_2O_3
AlMo-II–1.5%Li_2O	900	$Al_2(MoO_4)_3$ and α-Al_2O_3
AlMo-II–6%Li_2O	900	$Al_2(MoO_4)_3$, α-Al_2O_3 and Li_4MoO_5
AlMo-II	1000	α-Al_2O_3
AlMo-II–1.5%Li_2O	1000	α-Al_2O_3
AlMo-II–6%Li_2O	1000	α-Al_2O_3 and minute amounts of $Al_2(MoO_4)_3$

of these lines was found to increase by doping, indicating that Li_2O treatment enhanced the crystallization process of these phases and/or stimulated solid–solid interaction between MoO_3 and an alumina-producing aluminium molybdate compound. The absence of crystalline MoO_3 phase in AlMo-I solids preheated at 500°C could be attributed to monolayer dispersion of this oxide on the surface of the Al_2O_3 support [7–9, 11], and the increase in the amount of molybdenum trioxide present (AlMo-II solids) above the monolayer dispersion capacity (MLDC) of the Al_2O_3 support [7, 11] enhances the crystallization process of MoO_3 phase. The value of the MLDC of the employed Al_2O_3 support material towards MoO_3 can be readily calculated from the S_{BET} of Al_2O_3-500°C (188 $m^2\,g^{-1}$) and the amount of MoO_3 in AlMo-I solid (22 wt%). The value obtained was found to be 0.117 g of MoO_3 per 100 m^2 which is very close to the reported values [7, 11]. This value suggests a cross sectional area of 20.6 $Å^2$ per unit molybdate. The crystallization of MoO_3 phase can also be stimulated by increasing the calcination temperature of the supported oxide above 500°C which increases the surface and bulk mobilities of molybdenum species, leading to the formation of crystallized MoO_3 or $Al_2(MoO_4)_3$ compounds [5, 10]. The observed effect of Li_2O doping in increasing the crystallization of molybdenum trioxide and aluminium molybdate compounds at 500°C could be attributed to dissolution of a portion of Li_2O in MoO_3 lattice with subsequent increase in the mobility of the molybdenum species, especially those in the outermost surface layers of the oxide lattice [20, 21]. The stimulating effect of Li_2O in the crystallization of MoO_3 phase could also result from decreasing the monolayer dispersion capacity of the Al_2O_3 support due to location of lithium ions in octa- and tetrahedral sites of the alumina lattice [7, 22]. The formation of $Al_2(MoO_4)_3$ in the case of AlMo-II specimens calcined in air at 500°C took place via the following solid–solid interaction

$$3MoO_3 + Al_2O_3 \xrightarrow{500^\circ C} Al_2(MoO_4)_3$$

This reaction was not followed by any change in weight and took place at 500°C at a very slow rate that cannot be detected by a normal DTA technique (Fig. 2). The completion of this reaction thus requires the heating of various mixed oxide solids at higher temperatures.

Figs. 3 and 4 show the XRD patterns of pure and doped AlMo-I and AlMo-II solids preheated in air at 700°C. Fig. 3 shows that pure AlMo-I and that doped with 1.5 mol% Li_2O consist of well-crystallized $Al_2(MoO_4)_3$ and a mixture of γ- and κ-Al_2O_3 phases with moderate crystallinity, and the mixed solid sample treated with 6 mol% Li_2O consists of lithium aluminate $LiAl_5O_8$ (minute amount) as well as aluminium molybdate and a mixture of γ- and κ-aluminas.

The absence of all diffraction lines of MoO_3 phase in the patterns of the mixed oxides preheated at 700°C indicates its complete transformation into $Al_2(MoO_4)_3$. The fact that the pure alumina sample preheated at 700°C is an amorphous solid and is partly transformed into a mixture of κ- and γ-aluminas in the presence of molybdenum trioxide indicates the role of this oxide in catalysing the crystallization process of the treated alumina due to the formation of some kind of MoO_3–Al_2O_3 solid solution [11]. The formation of lithium aluminate in the 6 mol% Li_2O-doped mixed solid sample

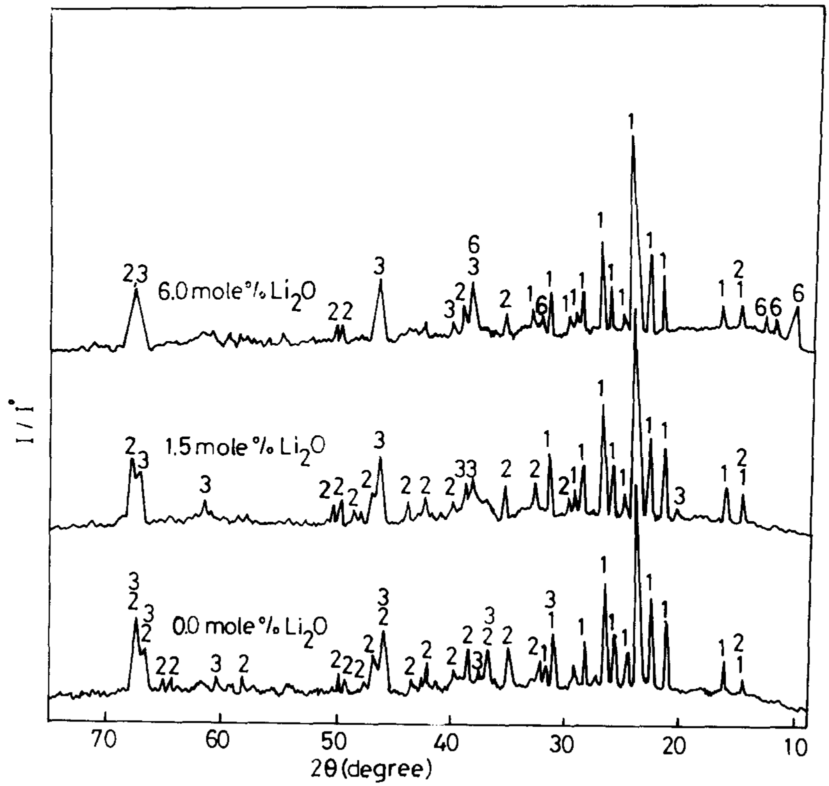

Fig. 3. X-ray diffractograms of pure and doped AlMo-I solids preheated in air at 700°C: 1, $Al_2(MoO_4)_3$; 2, κ-Al_2O_3; 3, γ-Al_2O_3; and 6, $LiAl_5O_8$ phases.

took place via the following solid–solid interaction

$$5Al_2O_3 + Li_2O \xrightarrow{700^\circ C} 2LiAl_5O_8$$

Fig. 4 shows that pure AlMo-II-700°C mixed solid sample consists of $Al_2(MoO_4)_2$ and δ-Al_2O_3 phases. It can also be seen from Fig. 4 that Li_2O doping enhanced the degree of crystallinity of the produced aluminium molybdate compound, as indicated from the considerable increase in the relative intensity of its diffraction lines. This effect could reflect an increase in the mobility of molybdenum species which facilitates diffusion in the alumina matrix, producing more ordered $Al_2(MoO_4)_3$ phase. Lithium oxide dissolved in MoO_3, similar to the case with NiO and V_2O_5 [20, 21, 23], might increase the mobility of molybdenum species. The formation of $LiAl_5O_8$ in AlMo-I and AlMo-II solids doped with 6 mol% Li_2O and calcined at 700°C, indicates a limited solubility of lithia in MoO_3 of the molybdenum–aluminium mixed oxide samples. The disappearance of all diffraction lines of δ-Al_2O_3 in all doped mixed oxide solids

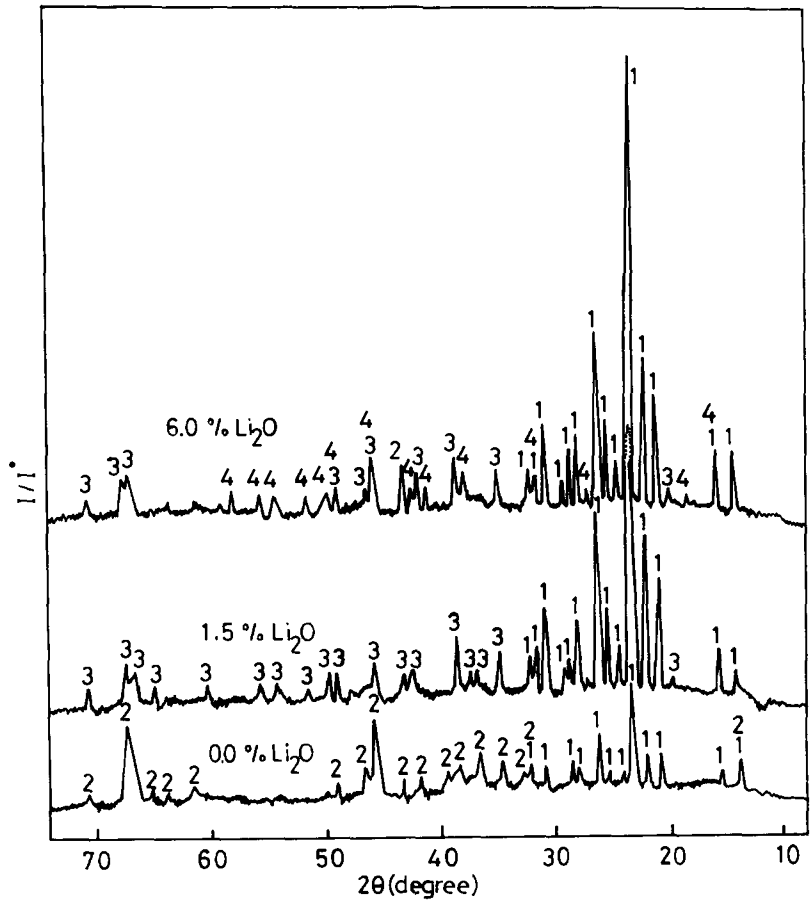

Fig. 4. X-ray diffractograms of pure and doped AlMo-II solids preheated in air at 700°C: 1, $Al_2(MoO_4)_3$; 2, δ-Al_2O_3; 3, κ-Al_2O_3; 4, $LiAl_5O_8$ phases.

preheated at 700°C indicates the role of Li_2O in catalysing the transformation of δ-Al_2O_3 into κ-alumina.

The aluminium molybdate compound formed in various pure and doped mixed solids can readily decompose by heating at temperatures above 700°C. The thermal stability of this compound can be monitored by the XRD analysis of different solids precalcined at 800–1000°C. Fig. 5 shows the diffractograms of pure and doped AlMo-II solids preheated at 1000°C. Table 3 shows that the pure AlMo-II-800°C specimen consists of a mixture of δ- and κ-aluminas together with a minute amount of undecomposed aluminium molybdate. These results indicate that most $Al_2(MoO_4)_3$ decomposed into MoO_3 and Al_2O_3 according to

$$Al_2(MoO_4)_3 \xrightarrow{800^\circ C} 3MoO_3 + Al_2O_3 \ (\delta\text{- and } \kappa\text{-forms})$$

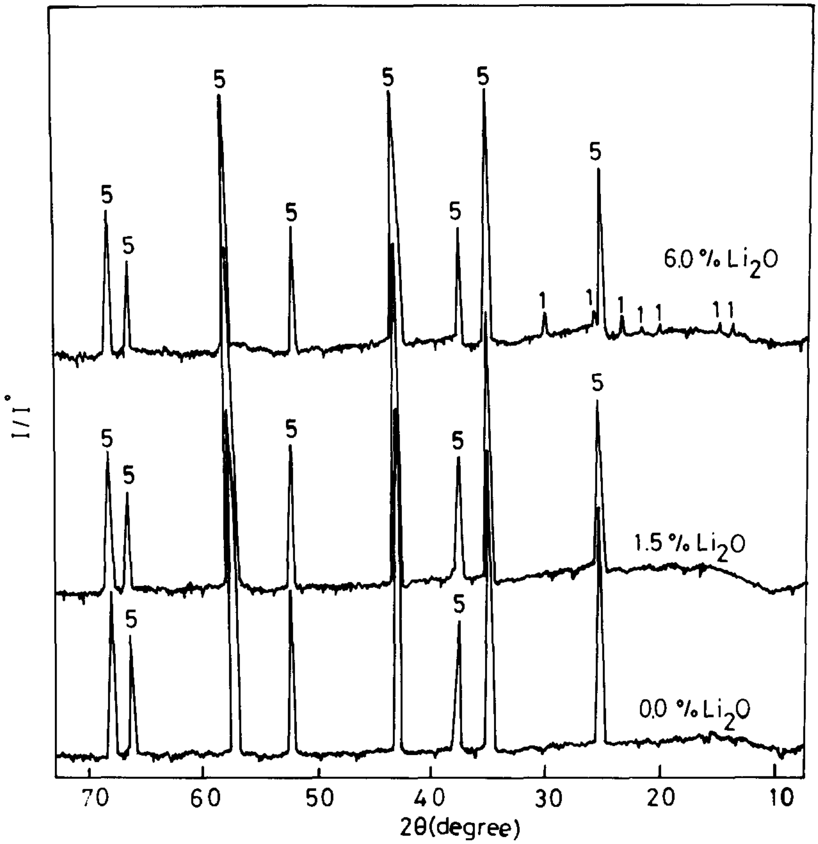

Fig. 5. X-ray diffractograms of pure and doped AlMo-II solids preheated in air at 1000°C; 1, $Al_2(MoO_4)_3$; 5, α-Al_2O_3 phases.

This reaction is not followed by any change in weight. It can be seen from XRD measurements that heating of Li_2O-doped material at 800°C resulted in a considerable increase in the relative intensity of all diffraction lines of $Al_2(MoO_4)_3$ phase and in the creation of new diffraction lines characteristic for α-Al_2O_3. The increase in the amount of Li_2O added to 6 mol% also resulted in the formation of lithium molybdate Li_4MoO_5, in addition to the complete tansformation of δ- and κ-aluminas into α-Al_2O_3. These results clearly indicate that: (i) Li_2O doping greatly enhanced the thermal stability of the $Al_2(MoO_4)_3$ compound; (ii) lithia catalysed the phase transformation Al_2O_3 (δ- and κ-phases) → α-Al_2O_3; (iii) a portion of Li_2O interacted with MoO_3 at 800°C yielding Li_4MoO_5 according to

$$2MoO_3 + 4Li_2O \xrightarrow{800\,C} 2Li_4MoO_5$$

The formation of lithium molybdate compound by heating the doped mixed solid specimen at 800°C suggests a limited solubility of Li_2O in MoO_3 lattice; (iv) the thermal decomposition of $Al_2(MoO_4)_3$ compound in the doped mixed solids required the thermal treatment of these solids at temperatures above 800°C.

It can also be seen from Table 3 that pure AlMo-II-900°C consists only of well-crystallized α-Al_2O_3, indicating the complete thermal decomposition of aluminium molybdate into α-alumina, with MoO_3 partly volatilized, and the remaining portion dissolved in the alumina matrix forming MoO_3–Al_2O_3 solid solution or buried in the bulk during the γ- $\rightarrow\alpha$-Al_2O_3 transformation.

The last endothermic peaks in the DTA curves of various investigated solids (Figs. 1 and 2) are indicative of partial sublimation of MoO_3 resulting from the thermal decomposition of the aluminium molybdate compound. It can also be observed from Table 3 that lithium oxide doping hindered the thermal decomposition of $Al_2(MoO_4)_3$ compound even on heating at 900°C. This effect was, however, more pronounced in the case of the AlMo-II-900°C specimen treated with 1.5 mol% Li_2O, probably due to the consuming of most of the added Li_2O (6 mol%) in the formation of Li_4MoO_5 compound. The rise in precalcination temperature of the doped mixed oxide solids to 1000°C might effect the complete thermal decomposition of the $Al_2(MoO_4)_3$ produced. Fig. 5 shows that pure and 1.5 mol% Li_2O-doped AlMo-II specimens preheated at 1000°C consist entirely of α-Al_2O_3, while the 6 mol% Li_2O-doped sample calcined in air at 1000°C still contained a small portion of undecomposed aluminium molybdate. The comparison of XRD diffractograms of pure and doped AlMo-II solids heated at 800 and 1000°C revealed that Li_4MoO_5 produced at 800°C decomposed readily at 1000°C. These results clearly indicate the role of Li_2O in increasing the thermal stability of aluminium molybdate even on heating at 1000°C and the catalysing effect in the transformation process of γ-, κ- and δ-aluminas into α-Al_2O_3 phase which took place at temperatures as low as 800°C. The different effects of Li_2O doping could be mainly attributed to a dissolution of a small amount (1.5 mol%) of Li_2O in the matrix of MoO_3 and Al_2O_3 solids, forming some kind of solid solution, with the subsequent increase in the mobilities of molybdenum and aluminium species. The possible increase in the mobilities of surface and bulk molybdenum and aluminium species favours the solid–solid interaction between Al_2O_3 and MoO_3, producing more ordered $Al_2(MoO_4)_3$ phase with relatively high thermal stability, and facilitates the crystallization process of aluminas into the stable α-Al_2O_3 form. The observed effect of Li_2O doping in decreasing the solubility of MoO_3 in the Al_2O_3 matrix (see Figs. 1 and 2) which is reflected in an enhanced increase in the volatility of MoO_3 from MoO_3–Al_2O_3 solid solution, might be taken as evidence for an induced increase in the mobility of molybdenum species in the MoO_3 lattice.

4. Conclusions

The main conclusions that can be derived from the obtained results are as follows:

1. Solid–solid interaction between MoO_3 and Al_2O_3 to produce $Al_2(MoO_4)_3$ took place at temperatures starting from 500°C, and its completion required the thermal treatment of the mixed oxide solids at 700°C. The presence of Li_2O enhanced the solid–solid interaction, yielding aluminium molybdate compound.

2. The aluminium molybdate produced decomposed by heating the pure mixed solids at temperatures starting from 850°C, giving MoO_3–Al_2O_3 solid solution. Li_2O doping decreased the solubility of MoO_3 in the alumina support material to an extent proportional to the amount of lithia present.

3. Lithium oxide doping of MoO_3–Al_2O_3 solids much increased the thermal stability of the aluminium molybdate compound produced, and a small portion of it remained stable even on heating at 1000°C.

4. Li_2O treatment of molybdenum/aluminium mixed oxides much enhanced the crystallization process of alumina into α-Al_2O_3 (corundum) at 800°C.

5. Li_2O interacted readily with Al_2O_3 and MoO_3 at 700 and 800°C to produce $LiAl_5O_8$ and Li_4MoO_5 compounds, respectively.

References

[1] Y. Okamato, T. Shimokaws, T. Imanka and S. Teranshi, J. Catal., 57 (1979) 153.
[2] P. Gajardo, P. Grang and B. Delmon, Surf. Interface Anal., 3 (1981) 206.
[3] A. Lycourghiotis, D. Vattis, G. Karaiskadis and N. Katsanos, J. Less-Common Met., 86 (1982) 137.
[4] M. Lo Jacono, M. Schiavello, V.H.J. De Beer and G. Minell, J. Phys. Chem., 81 (1977) 1583.
[5] R. Margraf, J. Leyrer, H. Knözinger and E. Taglauer, Surface Sci., 189/190 (1987) 842.
[6] H. Jeziorowski and H. Knözinger, J. Phys. Chem., 83 (1979) 1166.
[7] J. Leyrer, B. Vielhaber, M.I. Zaki, Z. Shuxian, J. Weitkamp and H. Knözinger, Mater. Chem. Phys., 13 (1985) 301.
[8] Y-J. Liu, Y-C. Xie, J. Liu and Y-Q. Tang, Cuihua Xuebao, 3 (1982) 262.
[9] Y-J. Liu, Y-C. Xie, C. Li, Z.-Y Zou and Y-Q. Tang, Cuihua Xuebao, 5 (1984) 234.
[10] R.C. McKenzie, Scifax Differential Thermal Analysis Data Index, Cleaver-Hume, London, 1962.
[11] A.A. Ibrahim and G.A. El-Shobaky, Thermochim. Acta, 147 (1989) 175.
[12] G.A. El-Shobaky, N.M. Ghoneim and E. Sultan, Thermochim. Acta, 63 (1983) 39.
[13] G.W. Brindly and J.O. Choe, Am. Mineral., 46 (1961) 771.
[14] J.A. Gadsen, IR Spectra of Minerals and Related Inorganic Compounds, Butterworths, London, 1975.
[15] G.A. El-Shobaky, N.H. Amin and G. Fagal, J. Radioanal. Nucl. Chem. Art., 177 (1994) 211; 178 (1994) 3.
[16] J. Zemlica and C. Barts, Krist Technol., 7 (1972) 965.
[17] G.A. El-Shobaky, K.A. El-Barawy and F.H.A. Abdalla, Thermochim. Acta, 96 (1985) 129.
[18] G.A. El-Shobaky, G.A. Fagal and A.M. Dessouki, Egypt. J. Chem., 31(3) (1983) 317.
[19] G.A. El-Shobaky, G.A. Fagal and N.H. Amin, Thermochim. Acta, 141 (1989) 205.
[20] P.C. Gravelle, G.A. El-Shobaky and S.J. Teichner, K. Hauffe and Th. Volkenstein (Eds.), Symp. Elect. Phenom. Chem. Catal., Walter de Gruter and Co., Berlin, 1969, p. 124.
[21] G.A. El-Shobaky, Surf. Technol., 7 (1978) 375.
[22] A. Lycourghiotis, C. Defosse, F. Delanary, J. Lemaitre and B. Delmon, J. Chem. Soc. Faraday Trans. 1., 76 (1980) 1677; 78 (1982) 1389.
[23] F.H.A. Abdalla, G.A. El-Shobaky and N.A. Hassan, Bull. Soc. Chim. Belg., 103(11) (1994) 665.